

# Search for New Physics in Rare Top Decays: $t\bar{t}$ Spin Correlations and Other Observables

Ken Kiers,<sup>1,\*</sup> Pratishruti Saha,<sup>2,†</sup> Alejandro Szynekman,<sup>3,‡</sup>  
David London,<sup>2,§</sup> Samuel Judge,<sup>1,¶</sup> and Jordan Melendez<sup>1,\*\*</sup>

<sup>1</sup>*Physics and Engineering Department, Taylor University,  
236 West Reade Ave., Upland, IN 46989, USA*

<sup>2</sup>*Physique des Particules, Université de Montréal,  
C.P. 6128, succ. centre-ville, Montréal, QC, Canada H3C 3J7*

<sup>3</sup>*IFLP, CONICET – Dpto. de Física, Universidad  
Nacional de La Plata, C.C. 67, 1900 La Plata, Argentina*

(Dated: October 2, 2015)

## Abstract

In this paper we study new-physics contributions to the top-quark decay  $t \rightarrow b\bar{b}c$ . We search for ways of detecting such new physics via measurements at the LHC. As top quarks are mainly produced at the LHC in  $t\bar{t}$  production via gluon fusion, we analyze the process  $gg \rightarrow t\bar{t} \rightarrow (b\bar{b}c)(\bar{b}\ell\bar{\nu})$ . We find six observables that can be used to reveal the presence of new physics in  $t \rightarrow b\bar{b}c$ . Three are invariant mass-squared distributions involving two of the final-state particles in the top decay, and three are angular correlations between the final-state quarks coming from the  $t$  decay and the  $\ell^-$  coming from the  $\bar{t}$  decay. The angular correlations are related to the  $t\bar{t}$  spin correlation.

PACS numbers: 14.65.Ha

---

\*Electronic address: knkiers@taylor.edu

†Electronic address: pratishruti.saha@umontreal.ca

‡Electronic address: szynkman@fisica.unlp.edu.ar

§Electronic address: london@lps.umontreal.ca

¶Electronic address: sdjudge@mtu.edu; Address after 9/1/2014: Department of Mathematics, Fisher Hall, Michigan Tech University, 1400 Townsend Drive, Houghton, Michigan 49931, USA.

\*\*Electronic address: jordan.melendez@taylor.edu

## I. INTRODUCTION

Physics beyond the standard model (SM) is expected to exist at energies above the weak scale. While successive experiments at LEP, the Tevatron and the LHC have served to validate the SM over the past few decades, no direct evidence of new physics (NP) has been found yet. Clearly, NP either exists at an energy scale higher than what has been probed, or its hints are subtler than we envision. The LHC, which is currently operational, is essentially a top-quark factory. The properties of the  $t$  can therefore be measured with good precision. Now, the mass of the top quark is more than an order of magnitude larger than that of all other fermions. As such, it may be affected by NP in ways that do not manifest themselves in the interactions of the lighter fermions. In addition, its large mass causes the top to decay before it can hadronize, so that it can be studied more or less as a free quark.

In this paper we study NP contributions to top-quark decay. The dominant  $t$  decay modes in the SM involve  $t \rightarrow W^+b$ , with  $W^+ \rightarrow \ell^+\nu_\ell$ ,  $u\bar{d}$  or  $c\bar{s}$ . Since the experimentally-measured value of the top decay width is in good agreement with the SM prediction [1], it is evident that the NP contribution to the dominant decay modes, if any, is very small compared to that of the SM. On the other hand, in the case of decay modes that are suppressed in the SM, an NP contribution that is comparable to that of the SM in that mode may go unnoticed simply because its impact on the total width is small. This makes it interesting to probe rare decays, as these could well be where the new physics is lurking. One such decay is  $t \rightarrow W^+b \rightarrow b\bar{b}c$ . It is suppressed in the SM because it involves the small element  $V_{cb}$  ( $\simeq 0.04$ ) of the Cabibbo-Kobayashi-Maskawa (CKM) quark mixing matrix. There are other suppressed decays (e.g.,  $t \rightarrow s\bar{s}c$ ), but here we focus on  $t \rightarrow b\bar{b}c$ .

Single-top production is rather suppressed at the LHC [2], so that it is difficult to isolate the decay  $t \rightarrow b\bar{b}c$  experimentally and analyze it on its own. The most significant production mode for top quarks at the LHC is pair ( $t\bar{t}$ ) production. At LHC energies, this is dominated by gluon fusion ( $gg \rightarrow t\bar{t}$ ), as opposed to quark-antiquark annihilation ( $q\bar{q} \rightarrow t\bar{t}$ ). In order to search for NP in top decay, the full process  $gg \rightarrow t\bar{t}$ , with  $t \rightarrow b\bar{b}c$  and  $\bar{t} \rightarrow \bar{b}\ell\bar{\nu}$ , must be analyzed. Apart from the usual difficulties of studying a multi-particle final state, this channel suffers from another complication – the  $\bar{t}$  decay leads to a second  $\bar{b}$  in the final state, providing an additional background that must be taken into account.

The main purpose of this paper is to analyze the process  $gg \rightarrow t(\rightarrow b\bar{b}c)\bar{t}(\rightarrow \bar{b}\ell\bar{\nu})$ , and to look for observables that can reveal the presence of NP in top decay<sup>1</sup>. We will show that there are two types of observables that can be used. The first is simply an invariant mass-squared distribution involving two of the final-state particles in  $t \rightarrow b\bar{b}c$ . With NP, its form is altered compared to that of the SM. Note, however, that this type of observable is entirely related to the decay of the  $t$  itself. The associated production of the  $\bar{t}$  is unimportant, except insofar that one must distinguish the  $\bar{b}$  quarks coming from the  $t$  and  $\bar{t}$  decays.

The second type of observable does rely on the fact that a  $t\bar{t}$  pair has been produced. The key point is that, in  $t\bar{t}$  production, the spins of the  $t$  and  $\bar{t}$  are correlated [5]. The

---

<sup>1</sup> Here we concentrate on CP-conserving observables. CP violation in  $t \rightarrow b\bar{b}c$ , along the lines of Ref. [3], will be examined elsewhere [4].

spin-correlation coefficient for the produced  $t\bar{t}$  pair can be defined as

$$\kappa_{t\bar{t}} = \frac{\sigma_{\uparrow\uparrow} + \sigma_{\downarrow\downarrow} - \sigma_{\uparrow\downarrow} - \sigma_{\downarrow\uparrow}}{\sigma_{\uparrow\uparrow} + \sigma_{\downarrow\downarrow} + \sigma_{\uparrow\downarrow} + \sigma_{\downarrow\uparrow}}, \quad (1)$$

where  $\uparrow$  and  $\downarrow$  denote the alignment of the spins of the top and antitop with respect to the chosen spin-quantization axis. The spin of the  $t$  itself is related to the angular distribution of its decay products through the relation

$$\frac{1}{\Gamma} \frac{d\Gamma}{d\cos\chi_i} = \frac{1}{2} (1 + \alpha_i \cos\chi_i), \quad (2)$$

where  $\chi_i$  is the angle between the direction of the  $i^{\text{th}}$  decay product and the spin quantization axis in the rest frame of the top, and  $\alpha_i$  is a numerical coefficient whose value depends on the identity of this decay product. The spin of the  $\bar{t}$  is related to the angular distribution of its decay products through a similar relation, with  $\chi_i \rightarrow \bar{\chi}_i$  and  $\alpha_i \rightarrow \bar{\alpha}_i$ . Naturally then, the spin correlation between the pair-produced top and antitop is manifested in the angular correlation between the decay products of the two particles. That relation is given as follows [6]:

$$\frac{1}{\sigma} \frac{d^2\sigma}{d\cos\chi_i d\cos\bar{\chi}_j} = \frac{1}{4} (1 + \kappa_{t\bar{t}} \alpha_i \bar{\alpha}_j \cos\chi_i \cos\bar{\chi}_j). \quad (3)$$

Its measurement permits the extraction of  $\kappa_{t\bar{t}}$ . If the measured value differs from the prediction of the SM, it would indicate the presence of NP.

One point should be noted at this juncture. The spin-correlation coefficient  $\kappa_{t\bar{t}}$  is, by definition, a property of the  $t\bar{t}$  production process. However, its experimental determination depends on the decay. Equation (3) assumes that the  $t$  and  $\bar{t}$  decay via SM interactions only. If there are NP contributions in top decay, the value of  $\kappa_{t\bar{t}}$  extracted from the angular correlations of the top and antitop decay products will be different from the SM prediction. This would not be due to a change in the value of  $\kappa_{t\bar{t}}$  itself, but rather to a change in the form of Eq. (3).

While there have been several studies of the effect of NP on  $t\bar{t}$  spin correlations, most of them have focused on NP that affects  $t\bar{t}$  production. These span both CP-conserving [7] and CP-violating [8] NP scenarios. Possibilities include non-standard  $gt\bar{t}$  couplings in the form of anomalous chromomagnetic dipole or chromoelectric dipole interactions, as well as many of the NP models proposed to explain the large  $t\bar{t}$  forward-backward asymmetry observed at the Tevatron [9].

Of course, NP contributions may be present in both  $t\bar{t}$  production and in the decay. However, NP in the production is much easier to detect, in that it should be observable even in the dominant decay modes of the top. For this reason we ignore the possibility of NP in  $t\bar{t}$  production in our analysis. We assume it will have been detected or ruled out before the study of NP in the decay is done.

Once the observables that carry the signature of NP have been pinpointed, the next question is: to what extent can they realistically be used to probe NP in top decay? Can they be used to identify, even partially, the type of NP present? This is examined in the companion paper [10]. There we show that it is likely that there will be enough events at

the LHC to measure these observables reasonably precisely and extract information about the nature of NP at play.

In this paper, we begin in Sec. II by examining how NP in top decay can affect  $t \rightarrow b\bar{b}c$ . In Sec. III we briefly discuss the full pair production and decay chain  $gg \rightarrow t\bar{t} \rightarrow (b\bar{b}c) (\bar{b}\ell\bar{\nu})$  (full details are given in the Appendix). The observables that can be used to search for NP in top decay are described in Sec. IV. In Sec. V we perform a numerical simulation of  $gg \rightarrow t\bar{t} \rightarrow (b\bar{b}c) (\bar{b}\ell\bar{\nu})$  at the LHC, including NP, and compare the results for the observables with our analytical calculations. We conclude in Sec. VI.

## II. NEW PHYSICS IN TOP DECAY

As detailed in the introduction, this work focuses on the search for new physics in rare decays of the top quark. In this paper, we examine the decay  $t \rightarrow b\bar{b}c$ . However, the method described here can also be applied to other suppressed decays such as  $t \rightarrow s\bar{s}c$ , etc.

While examining a suppressed decay mode, one must consider the most dominant production mode in order to have sufficient statistics. Hence, the search for NP in this top decay mode must involve the process  $gg \rightarrow t\bar{t}$ . Even there, one may have chosen to ignore the details of the production process and focus only on the decay. However, as we show in the following sections, there is something to be gained by considering the full process  $gg \rightarrow t\bar{t} \rightarrow (b\bar{b}c) (\bar{b}\ell\bar{\nu})$ , in that the  $t\bar{t}$  spin correlations can be put to use in the identification of NP.

### A. $t \rightarrow b\bar{b}c$ : effective Lagrangian

In the SM, the decay  $t \rightarrow b\bar{b}c$  arises via  $t \rightarrow W^+b$ , followed by  $W^+ \rightarrow \bar{b}c$ . NP contributions to  $t \rightarrow b\bar{b}c$  can be parameterized via an effective Lagrangian  $\mathcal{L}_{\text{eff}} = \mathcal{L}_{\text{eff}}^V + \mathcal{L}_{\text{eff}}^S + \mathcal{L}_{\text{eff}}^T$ , with

$$\begin{aligned} \mathcal{L}_{\text{eff}}^V = & 4\sqrt{2}G_F V_{cb}V_{tb} \left\{ X_{LL}^V \bar{b}\gamma_\mu P_L t \bar{c}\gamma^\mu P_L b + X_{LR}^V \bar{b}\gamma_\mu P_L t \bar{c}\gamma^\mu P_R b \right. \\ & \left. + X_{RL}^V \bar{b}\gamma_\mu P_R t \bar{c}\gamma^\mu P_L b + X_{RR}^V \bar{b}\gamma_\mu P_R t \bar{c}\gamma^\mu P_R b \right\} + \text{h.c.}, \end{aligned} \quad (4)$$

$$\begin{aligned} \mathcal{L}_{\text{eff}}^S = & 4\sqrt{2}G_F V_{cb}V_{tb} \left\{ X_{LL}^S \bar{b}P_L t \bar{c}P_L b + X_{LR}^S \bar{b}P_L t \bar{c}P_R b \right. \\ & \left. + X_{RL}^S \bar{b}P_R t \bar{c}P_L b + X_{RR}^S \bar{b}P_R t \bar{c}P_R b \right\} + \text{h.c.}, \end{aligned} \quad (5)$$

$$\begin{aligned} \mathcal{L}_{\text{eff}}^T = & 4\sqrt{2}G_F V_{cb}V_{tb} \left\{ X_{LL}^T \bar{b}\sigma^{\mu\nu} P_L t \bar{c}\sigma_{\mu\nu} P_L b \right. \\ & \left. + X_{RR}^T \bar{b}\sigma^{\mu\nu} P_R t \bar{c}\sigma_{\mu\nu} P_R b \right\} + \text{h.c.} \end{aligned} \quad (6)$$

In the above expressions, colour indices are not shown, but are assumed to contract in the same manner as those of the SM (i.e., the fields  $\bar{b}$  with  $t$  and  $\bar{c}$  with  $b$ ). In some NP models, the colour indices would contract in the opposite manner (i.e., the fields  $\bar{c}$  with  $t$  and  $\bar{b}$  with  $b$ ). However, with Fierz transformations it is straightforward to incorporate colour-mismatched terms into the effective Lagrangian [3].

In general, the NP couplings (the  $X$ 's in the above equations) have both weak and strong phases. However, as argued in Ref. [11], since the NP strong phases can only be generated by self-rescattering from the NP operators, they are very small. For this reason, we neglect all NP strong phases, so that the  $X$ 's contain only weak phases. Furthermore, the NP couplings can all reasonably be assumed to be of order unity, so that the SM and NP contributions to  $t \rightarrow b\bar{b}c$  can very well be about the same size. When computing the effect of NP on a particular observable, it is therefore important to include both the SM-NP and NP-NP interference pieces.

## B. $t \rightarrow b\bar{b}c$ : $|\mathcal{M}|^2$

We calculate the square of the matrix element for  $t \rightarrow b\bar{b}c$  as a function of the top-quark spin ( $s_t$ ), including the SM and all the NP contributions. We find

$$\frac{1}{3} \sum_{\substack{\text{colours,} \\ b, \bar{b}, c \text{ spins}}} |\mathcal{M}(t(s_t) \rightarrow b\bar{b}c)|^2 = 96G_F^2 m_t (V_{tb}V_{cb})^2 \left[ \sum_{i, \sigma} A_i^\sigma \left( \frac{p_i \cdot p_t}{m_t} - \xi^\sigma p_i \cdot s_t \right) - 16 \text{Im} (X_{LL}^T X_{LL}^{S*} + X_{RR}^T X_{RR}^{S*}) \epsilon(p_t, s_t, p_{\bar{b}}, p_c) \right], \quad (7)$$

where  $\epsilon(p_t, s_t, p_{\bar{b}}, p_c) \equiv \epsilon_{\mu\nu\rho\sigma} p_t^\mu s_t^\nu p_{\bar{b}}^\rho p_c^\sigma$ , with  $\epsilon_{0123} = -1$  and where  $s_t$  is the spin four-vector of the top quark. Above,  $\sigma = \pm$ ,  $\xi^\pm = \pm 1$  and  $i = \bar{b}, b, c$ .  $A_{\bar{b}}^\pm$  is defined as

$$A_{\bar{b}}^\pm = (p_t - p_{\bar{b}})^2 \left[ m_W^4 |G_T|^2 + 4m_W^2 \text{Re}(G_T X_{LL}^{V*}) + \hat{A}_{\bar{b}}^\pm \right], \quad (8)$$

where  $G_T \equiv G_T(q^2) = (q^2 - M_W^2 + i\Gamma_W M_W)^{-1}$  and  $q^2 = 2p_{\bar{b}} \cdot p_c$ . The remaining  $A_i^\sigma$  are defined as

$$A_i^\sigma = (p_t - p_i)^2 \hat{A}_i^\sigma, \quad (\text{all } i, \sigma, \text{ except } i = \bar{b}, \sigma = +). \quad (9)$$

In the above,

$$\begin{aligned} \hat{A}_{\bar{b}}^+ &= 4 |X_{LL}^V|^2 - 8 \text{Re}(X_{LL}^T X_{LL}^{S*}) + 32 |X_{LL}^T|^2, \\ \hat{A}_{\bar{b}}^- &= 4 |X_{RR}^V|^2 - 8 \text{Re}(X_{RR}^T X_{RR}^{S*}) + 32 |X_{RR}^T|^2, \\ \hat{A}_b^+ &= |X_{LL}^S|^2 + |X_{LR}^S|^2 - 16 |X_{LL}^T|^2, \\ \hat{A}_b^- &= |X_{RR}^S|^2 + |X_{RL}^S|^2 - 16 |X_{RR}^T|^2, \\ \hat{A}_c^+ &= 4 |X_{LR}^V|^2 + 8 \text{Re}(X_{LL}^T X_{LL}^{S*}) + 32 |X_{LL}^T|^2, \\ \hat{A}_c^- &= 4 |X_{RL}^V|^2 + 8 \text{Re}(X_{RR}^T X_{RR}^{S*}) + 32 |X_{RR}^T|^2. \end{aligned} \quad (10)$$

Note that  $A_{\bar{b}}^\pm$  contains both the SM and NP contributions, whereas the other  $A_i^\sigma$  contain only NP contributions.

The term proportional to  $\epsilon(p_t, s_t, p_{\bar{b}}, p_c)$  in Eq. (7) describes the triple product (TP) in the decay. Because the  $X$ 's contain only weak phases, the TP is purely CP-violating. Furthermore, Eq. (8) contains terms proportional to  $\text{Re}(G_T)\text{Re}(X_{LL}^{V*})$  and  $\text{Im}(G_T)\text{Im}(X_{LL}^{V*})$ . Of these,  $\text{Im}(G_T)\text{Im}(X_{LL}^{V*})$  is also CP-violating. Now, if one adds Eq. (7) to its CP-conjugate counterpart, all CP-violating terms cancel, leaving the remaining terms unchanged (apart from a normalization factor of 1/2). In focusing on CP-conserving observables, we implicitly assume that this CP averaging has been performed.

The main point to be retained from Eq. (7) is that the amplitude squared depends on seven different combinations of NP couplings – six  $\hat{A}_i^\sigma$ 's and  $\text{Re}(X_{LL}^{V*})$ . Thus, there are a number of independent observables that, in principle, can provide information about the NP. While we can hope to measure all seven of these quantities, we cannot measure all of the individual  $X$  parameters. In the remainder of this paper (and in the companion paper), when we refer to “identifying” the NP, what is meant is this partial identification of the six  $\hat{A}_i^\sigma$ 's and  $\text{Re}(X_{LL}^{V*})$ , not the complete identification of all of the  $X$  parameters.

### III. $gg \rightarrow t\bar{t} \rightarrow (b\bar{b}c)(\bar{b}\ell\bar{\nu})$

As a first step, we calculate the cross-section for  $t\bar{t}$  pair production followed by the decay chain  $t \rightarrow b\bar{b}c$ ,  $\bar{t} \rightarrow \bar{b}\ell\bar{\nu}$ . We present an outline of the analysis in what follows; the more technical details can be found in the Appendix.

Briefly, the analysis proceeds as follows. The process is represented in Fig. 1. The six-body phase space is decomposed into five solid angles and four invariant masses. The narrow-width approximation<sup>2</sup> is then used for the  $t$  and  $\bar{t}$  quarks to eliminate two of the invariant-mass degrees of freedom. The solid angles  $d\Omega_1^{**}$ ,  $d\Omega_2^*$ ,  $d\Omega_4^{**}$ ,  $d\Omega_5^*$  and  $d\Omega_t$  are defined in five different rest frames, as indicated in Fig. 1. The  $*$  and  $**$  superscripts indicate that these angles are defined in reference frames that are, respectively, one and two boosts away from the  $t\bar{t}$  rest frame. The invariant masses  $M_2$  and  $M_5$  are defined through the relations  $M_2^2 = (p_1 + p_2)^2$  and  $M_5^2 = (p_4 + p_5)^2$ . In the end, the differential cross section is a complicated function of the final-state momenta  $p_i$  ( $i = 1-6$ ) and the couplings, and is defined with respect to  $dM_2^2 dM_5^2 d\Omega_1^{**} d\Omega_2^* d\Omega_4^{**} d\Omega_5^* d\Omega_t$ .

We stress that Fig. 1 represents only the kinematics of  $gg \rightarrow t\bar{t} \rightarrow (b\bar{b}c)(\bar{b}\ell\bar{\nu})$ . It is not a Feynman diagram. In particular,  $M_5^2$  does not necessarily correspond to the  $W^-$  resonance in the  $\bar{t}$  decay, and  $M_2^2$  does not necessarily correspond to the  $W^+$  resonance in the SM part of the  $t$  decay. Rather,  $p_1$ ,  $p_2$  and  $p_3$  are the momenta of the  $b$ ,  $\bar{b}$  and  $c$  quarks in  $t \rightarrow b\bar{b}c$ , with all permutations being allowed. That is,  $p_1$ ,  $p_2$  and  $p_3$  can each stand for  $p_b$ ,  $p_{\bar{b}}$  or  $p_c$ , and similarly for the particles in the  $\bar{t}$  decay. In constructing the observables, we consider several of these possibilities.

---

<sup>2</sup> The narrow-width approximation is equivalent to assuming that the decaying particle is on-shell. Throughout the paper, we apply this to the  $t$  and  $\bar{t}$  quarks produced via gluon fusion, to the  $W$  produced in the  $\bar{t}$  decay, and generally to the  $W$  produced in the  $t$  decay.

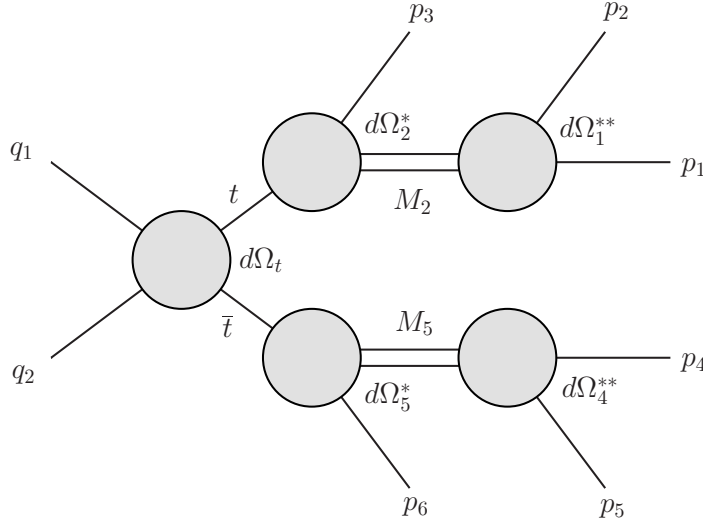


FIG. 1: Kinematics for the process  $gg \rightarrow t\bar{t} \rightarrow (b\bar{b}c)(\bar{b}l\bar{\nu})$  [12].  $\Omega_1^{**}$  denotes the direction of  $\vec{p}_1^{**}$  in the rest frame of  $M_2$ , relative to the direction of  $\vec{p}_1^* + \vec{p}_2^*$ , where  $M_2^2 = (p_1 + p_2)^2$ . Similarly,  $\Omega_2^*$  denotes the direction of  $(\vec{p}_1^* + \vec{p}_2^*)$  in the  $t$  rest frame, relative to the direction of  $\vec{p}_t$  in the  $t\bar{t}$  rest frame.  $\Omega_t$  denotes the direction of  $\vec{p}_t$  relative to  $\vec{q}_1$ , also in the  $t\bar{t}$  rest frame. The solid angles  $\Omega_4^{**}$  and  $\Omega_5^*$  are defined analogously to  $\Omega_1^{**}$  and  $\Omega_2^*$ , respectively, and  $M_5^2 = (p_4 + p_5)^2$ .

#### IV. OBSERVABLES

The first step in finding observables that can yield information about NP in top decay is to define which final-state particles correspond to  $p_1$ - $p_6$ . There are several choices possible, corresponding to different observables. Throughout this work the momenta for the  $\bar{t}$  decay products are assigned as follows:  $p_4 = p_{\bar{\nu}}$ ,  $p_5 = p_{\bar{b}}$  and  $p_6 = p_{\ell}$ . Taking  $p_1 = p_c$ ,  $p_2 = p_b$  and integrating Eq. (56) from the Appendix over  $M_5^2$  and over all angles except  $\theta_b^*$  and  $\theta_\ell^*$ , we find<sup>3</sup>

$$\begin{aligned} & \frac{d\sigma}{d\cos\theta_b^* d\cos\theta_\ell^* d\zeta_{bc}^2} \\ &= \frac{\sigma_{\text{SM}}}{4} \left\{ \frac{6 h_{\text{SM}}^{bc} (\zeta_{bc}^2)}{(1 - \zeta_W^2)^2 (1 + 2\zeta_W^2)} [1 + \kappa(r) \cos\theta_b^* \cos\theta_\ell^*] \right. \\ & \quad \left. + \frac{3G_F m_t^2}{\sqrt{2}\pi^2 (1 - \zeta_W^2)^2 (1 + 2\zeta_W^2)} \sum_{i,\sigma} \hat{A}_i^\sigma \left[ h_i^{bc}(\zeta_{bc}^2) + \tilde{h}_i^{bc}(\zeta_{bc}^2) \xi^\sigma \kappa(r) \cos\theta_b^* \cos\theta_\ell^* \right] \right\}, \quad (11) \end{aligned}$$

<sup>3</sup> The angle  $\theta_b^*$  is “ $\theta_2^*$ ” in this case (see the caption of Fig. 1 for a precise definition). This angle is associated with the direction of the  $b$ - $c$  center of mass in the top rest frame, which is opposite to the direction of the  $\bar{b}$  in this frame. Similarly,  $\theta_\ell^*$  is “ $\theta_5^*$ ”.

where  $\zeta_{bc}^2 \equiv (p_b + p_c)^2 / m_t^2$  and  $\zeta_W \equiv m_W / m_t$ .  $\sigma_{SM}$  is defined in Eq. (60) of the Appendix, the  $\hat{A}_i^\sigma$ 's are given in Eq. (10), and  $\kappa(r)$  is defined as

$$\kappa(r) = \frac{(-31r^4 + 37r^2 - 66)r - 2(r^6 - 17r^4 + 33r^2 - 33)\tanh^{-1}(r)}{r^2[(31r^2 - 59)r + 2(r^4 - 18r^2 + 33)\tanh^{-1}(r)]}, \quad (12)$$

where  $r$  is defined in Eq. (27) in the Appendix. Note that  $\langle \kappa(r) \rangle = -\kappa_{t\bar{t}}$  as defined in Eq. (1). The functions  $h_i^{bc}(\zeta_{bc}^2)$  and  $\tilde{h}_i^{bc}$  are defined in Table I, and

$$h_{SM}^{bc}(\zeta_{bc}^2) = (1 - \zeta_{bc}^2) \zeta_{bc}^2 \theta(1 - \zeta_W^2 - \zeta_{bc}^2). \quad (13)$$

In writing down Eq. (11), we have dropped a contribution proportional to  $\text{Re}(X_{LL}^{V*})$ , which tends to yield a somewhat small effect in practice. This contribution is not difficult to calculate, but its inclusion makes the expression for the differential cross section somewhat cumbersome. Also, since we are only considering CP-even contributions, we have dropped a term proportional to  $\text{Im}(X_{LL}^{V*})$ .

TABLE I: Definitions of the  $h_i^{mn}$  ( $mn = bc, \bar{b}c, b\bar{b}$ ) and  $\tilde{h}_i^{bc}$  functions. The columns correspond to  $i = b, \bar{b}, c$ .

	$b$	$\bar{b}$	$c$
$h_i^{bc}(\zeta^2)$	$\frac{1}{2}(1 - \zeta^2)^2(1 + 2\zeta^2)$	$3(1 - \zeta^2)^2\zeta^2$	$\frac{1}{2}(1 - \zeta^2)^2(1 + 2\zeta^2)$
$\tilde{h}_i^{bc}$	$-\frac{1}{2}(1 - \zeta^2)^2(1 - 2\zeta^2)$	$3(1 - \zeta^2)^2\zeta^2$	$-\frac{1}{2}(1 - \zeta^2)^2(1 - 2\zeta^2)$
$h_i^{\bar{b}c}(\zeta^2)$	$3(1 - \zeta^2)^2\zeta^2$	$\frac{1}{2}(1 - \zeta^2)^2(1 + 2\zeta^2)$	$\frac{1}{2}(1 - \zeta^2)^2(1 + 2\zeta^2)$
$h_i^{b\bar{b}}(\zeta^2)$	$\frac{1}{2}(1 - \zeta^2)^2(1 + 2\zeta^2)$	$\frac{1}{2}(1 - \zeta^2)^2(1 + 2\zeta^2)$	$3(1 - \zeta^2)^2\zeta^2$

Starting from Eq. (11), we can integrate one or two more times to obtain differential cross sections in terms of the two angles or in terms of the invariant mass squared, respectively. These are the two types of observables we focus on in this paper:

**Invariant mass-squared distribution.** Integrating over the angles  $\theta_{\bar{b}}^*$  and  $\theta_\ell^*$  in Eq. (11) yields

$$\frac{d\sigma}{d\zeta_{bc}^2} = \sigma_{SM} \left\{ \frac{6 h_{SM}^{bc}(\zeta_{bc}^2)}{(1 - \zeta_W^2)^2 (1 + 2\zeta_W^2)} + \frac{3G_F m_t^2}{\sqrt{2}\pi^2 (1 - \zeta_W^2)^2 (1 + 2\zeta_W^2)} \sum_{i,\sigma} \hat{A}_i^\sigma h_i^{bc}(\zeta_{bc}^2) \right\}. \quad (14)$$

The above contains three functions of  $\zeta_{bc}^2$  that multiply the various SM and NP terms:  $h_{SM}^{bc}$ ,  $h_{\bar{b}}^{bc}$  and  $h_b^{bc} = h_c^{bc}$ . The three functions are qualitatively different from each other, so that the measurement of the invariant mass-squared distribution permits the extraction of the NP parameters  $\hat{A}_b^+ + \hat{A}_{\bar{b}}^-$  and  $\hat{A}_b^+ + \hat{A}_{\bar{b}}^- + \hat{A}_c^+ + \hat{A}_c^-$ .



**Angular correlation.** Integrating over  $\zeta_{bc}^2$  in Eq. (11), we obtain

$$\begin{aligned} \frac{d\sigma}{d\cos\theta_b^* d\cos\theta_\ell^*} &= \frac{\sigma_{\text{SM}}}{4} \left\{ [1 + \kappa(r) \cos\theta_b^* \cos\theta_\ell^*] \right. \\ &+ \frac{3G_F m_t^2}{4\sqrt{2}\pi^2 (1 - \zeta_W^2)^2 (1 + 2\zeta_W^2)} \left[ \left( \sum_{i,\sigma} \hat{A}_i^\sigma \right) \right. \\ &\left. \left. + \left( \hat{A}_b^+ - \hat{A}_b^- - \frac{1}{3} (\hat{A}_b^+ - \hat{A}_b^- + \hat{A}_c^+ - \hat{A}_c^-) \right) \kappa(r) \cos\theta_b^* \cos\theta_\ell^* \right] \right\}. \end{aligned} \quad (15)$$

By measuring this differential cross section and comparing it to the SM prediction, one can extract the sum of NP parameters  $\sum_{i,\sigma} \hat{A}_i^\sigma$  and a linear combination of the differences  $\hat{A}_i^+ - \hat{A}_i^-$  ( $i = \bar{b}, b, c$ ). Note that this observable is sensitive to the  $t\bar{t}$  spin correlation. For the SM, this is just the coefficient of the term proportional to  $\cos\theta_b^* \cos\theta_\ell^*$ , up to an overall normalization factor. Once NP is included, this term gets an additional contribution proportional to a combination of differences of the NP parameters.

It is straightforward to perform the above analysis for the two other invariant masses and angles in the  $t$  decay. Taking  $p_1 = p_c$  and  $p_2 = p_{\bar{b}}$ , we have

$$\begin{aligned} \frac{d\sigma}{d\zeta_{bc}^2} &= \sigma_{\text{SM}} \left\{ [1 - 4(1 - \zeta_{bc}^2/\zeta_W^2) \text{Re}(X_{LL}^{V*})] \frac{6 h_{\text{SM}}^{\bar{b}c}(\zeta_{bc}^2)}{(1 - \zeta_W^2)^2 (1 + 2\zeta_W^2)} \right. \\ &\left. + \frac{3G_F m_t^2}{\sqrt{2}\pi^2 (1 - \zeta_W^2)^2 (1 + 2\zeta_W^2)} \sum_{i,\sigma} \hat{A}_i^\sigma h_i^{\bar{b}c}(\zeta_{bc}^2) \right\}, \end{aligned} \quad (16)$$

where the  $h_i^{\bar{b}c}$  are defined in Table I and

$$h_{\text{SM}}^{\bar{b}c}(\zeta_{bc}^2) = \left( \frac{\zeta_W \gamma_W}{6\pi} \right) \frac{(1 - \zeta_{bc}^2)^2 (1 + 2\zeta_{bc}^2)}{(\zeta_{bc}^2 - \zeta_W^2)^2 + (\zeta_W \gamma_W)^2}, \quad (17)$$

with  $\gamma_W = \Gamma_W/m_t$ . Here, since  $h_b^{\bar{b}c}$  is different from  $h_c^{\bar{b}c} = h_c^{\bar{b}c}$ , the measurement of the invariant mass-squared distribution permits the extraction of the NP parameters  $\hat{A}_b^+ + \hat{A}_b^-$  and  $\hat{A}_b^+ + \hat{A}_b^- + \hat{A}_c^+ + \hat{A}_c^-$ , as well as  $\text{Re}(X_{LL}^{V*})$ .

The corresponding angular correlation is given by

$$\begin{aligned} \frac{d\sigma}{d\cos\theta_b^* d\cos\theta_\ell^*} &= \frac{\sigma_{\text{SM}}}{4} \left\{ [1 + \rho_b(\zeta_W^2) \kappa(r) \cos\theta_b^* \cos\theta_\ell^*] \right. \\ &+ \frac{3G_F m_t^2}{4\sqrt{2}\pi^2 (1 - \zeta_W^2)^2 (1 + 2\zeta_W^2)} \left[ \left( \sum_{i,\sigma} \hat{A}_i^\sigma \right) \right. \\ &\left. \left. + \left( \hat{A}_b^+ - \hat{A}_b^- - \frac{1}{3} (\hat{A}_b^+ - \hat{A}_b^- + \hat{A}_c^+ - \hat{A}_c^-) \right) \kappa(r) \cos\theta_b^* \cos\theta_\ell^* \right] \right\}, \end{aligned} \quad (18)$$

where

$$\rho_b(\zeta_W^2) = - \left( \frac{1 - 2\zeta_W^2}{1 + 2\zeta_W^2} \right). \quad (19)$$

The measurement of this angular correlation allows one to extract the sum of NP parameters  $\sum_{i,\sigma} \hat{A}_i^\sigma$  and a different linear combination of the differences  $\hat{A}_i^+ - \hat{A}_i^-$  ( $i = \bar{b}, b, c$ ) as compared to Eq. (15).

Finally, we take  $p_1 = p_b$  and  $p_2 = p_{\bar{b}}$ . In this case,

$$\begin{aligned} \frac{d\sigma}{d\zeta_{b\bar{b}}^2} = \sigma_{\text{SM}} \left\{ \frac{6 h_{\text{SM}}^{b\bar{b}}(\zeta_{b\bar{b}}^2)}{(1 - \zeta_W^2)^2 (1 + 2\zeta_W^2)} \right. \\ \left. + \frac{3G_F m_t^2}{\sqrt{2}\pi^2 (1 - \zeta_W^2)^2 (1 + 2\zeta_W^2)} \sum_{i,\sigma} \hat{A}_i^\sigma h_i^{b\bar{b}}(\zeta_{b\bar{b}}^2) \right\}, \quad (20) \end{aligned}$$

where the  $h_i^{b\bar{b}}$  are defined in Table I, and

$$h_{\text{SM}}^{b\bar{b}}(\zeta_{b\bar{b}}^2) = (1 - \zeta_W^2 - \zeta_{b\bar{b}}^2) (\zeta_W^2 + \zeta_{b\bar{b}}^2) \theta(1 - \zeta_W^2 - \zeta_{b\bar{b}}^2). \quad (21)$$

We have dropped a contribution proportional to  $\text{Re}(X_{LL}^{V*})$  in Eq. (20), because its effect is somewhat small in practice. The measurement of the invariant mass-squared distribution permits the extraction of the NP parameters  $\hat{A}_c^+ + \hat{A}_c^-$  and  $\hat{A}_b^+ + \hat{A}_b^- + \hat{A}_{\bar{b}}^+ + \hat{A}_{\bar{b}}^-$ .

The angular correlation is given by

$$\begin{aligned} \frac{d\sigma}{d\cos\theta_c^* d\cos\theta_\ell^*} = \frac{\sigma_{\text{SM}}}{4} \left\{ [1 + \rho_c(\zeta_W^2) \kappa(r) \cos\theta_c^* \cos\theta_\ell^*] \right. \\ \left. + \frac{3G_F m_t^2}{4\sqrt{2}\pi^2 (1 - \zeta_W^2)^2 (1 + 2\zeta_W^2)} \left[ \left( \sum_{i,\sigma} \hat{A}_i^\sigma \right) \right. \right. \\ \left. \left. + \left( \hat{A}_c^+ - \hat{A}_c^- - \frac{1}{3} (\hat{A}_b^+ - \hat{A}_b^- + \hat{A}_{\bar{b}}^+ - \hat{A}_{\bar{b}}^-) \right) \kappa(r) \cos\theta_c^* \cos\theta_\ell^* \right] \right\}, \quad (22) \end{aligned}$$

where

$$\rho_c(\zeta_W^2) = \frac{1 - 12\zeta_W^2 + 9\zeta_W^4 + 2\zeta_W^6 - 12\zeta_W^4 \ln(\zeta_W^2)}{(1 - \zeta_W^2)^2 (1 + 2\zeta_W^2)}. \quad (23)$$

Here the measurement of the angular correlation allows one to extract the sum of NP parameters  $\sum_{i,\sigma} \hat{A}_i^\sigma$  and a third distinct linear combination of the differences  $\hat{A}_i^+ - \hat{A}_i^-$  ( $i = \bar{b}, b, c$ ).

The measurement of any of these observables allows one to detect the presence of NP in top decay. If all three angular correlations and invariant mass-squared distributions can be

measured, the results can be combined to give measurements of all six NP parameters  $\hat{A}_i^\sigma$ , as well as  $\text{Re}(X_{LL}^{V*})$ . Furthermore, there are numerous measurements, providing significant redundancy. This is discussed in detail in the companion paper, Ref. [10].

One can also perform all of the integrations, giving the total cross section [3]:

$$\sigma = \sigma_{\text{SM}} \left\{ 1 + \frac{3G_F m_t^2}{4\sqrt{2}\pi^2 (1 - \zeta_W^2)^2 (1 + 2\zeta_W^2)} \sum_{i,\sigma} \hat{A}_i^\sigma \right\}. \quad (24)$$

The measurement of  $\sigma$  is, in principle, the most straightforward way to detect NP. Any disagreement between the measured total cross section and its SM value would indicate NP. The downside of this approach, however, is that the absolute size of the cross section might be difficult to determine due to QCD corrections, etc.<sup>4</sup> For this reason it may be better to use the invariant mass-squared distributions and/or the angular correlations.

The measurement of the triple-differential distribution of Eq. (11) would give a great deal of information about the NP parameters. However, it is unlikely there will be sufficient statistics to allow this measurement to be carried out.

## V. NUMERICAL SIMULATION

The expressions in the previous section provide a clear picture of the corrections to the various observables introduced by the new-physics contributions. In order to obtain meaningful projections in the context of the LHC, we perform a numerical simulation using MadGraph 5 [14]. The new couplings due to the effective Lagrangian [Eqs. (4)-(6)] are incorporated into MadGraph 5 via FeynRules [15]. We compute  $gg \rightarrow t\bar{t} \rightarrow (b\bar{b}c)(\bar{b}e^-\bar{\nu}_e)$  and obtain the  $d\sigma/d\zeta_{ij}^2$  distributions and the angular correlations discussed in the previous section. This naturally involves the convolution of the cross sections and differential cross sections calculated at the parton level with the appropriate parton densities. We use CTEQ6L1 PDFs [16] with the factorization and renormalization scales set to  $m_t = 172$  GeV.

In Fig. 2, we compare the normalized  $d\sigma/d\zeta_{bc}^2$  distribution obtained using MadGraph 5 for a  $pp$  collider with a centre-of-mass energy of 14 TeV with that obtained for gluons colliding at a fixed centre-of-mass energy of 600 GeV using the analytic expression in Eq. (14). This is done for both the SM and a particular NP scenario<sup>5</sup>. In both cases there is remarkable agreement between the two methods of obtaining  $d\sigma/d\zeta_{bc}^2$ . At first glance, this may seem extremely surprising, but a slightly closer look at the issue reveals that it is not really so.

The  $d\sigma/d\zeta_{ij}^2$  distributions involve only the decay products of the top. Any observable that involves only particles coming from a single decay can be computed in the rest frame of

<sup>4</sup> Theoretical calculations of the cross section for  $t\bar{t}$  pair production can be found in Ref. [13]. These include contributions from both  $gg$  and  $q\bar{q}$ , as well as higher-order corrections. The  $t\bar{t}$  cross section at the LHC at a centre-of-mass energy of 14 TeV is  $\sim 900$  pb.

<sup>5</sup> We take  $X_{RR}^S = X_{RR}^V = X_{RR}^T = 1 + i$ . Note that, although these NP parameters are complex, there are no SM-NP or NP-NP interference effects. As such, they do not lead to CP violation.

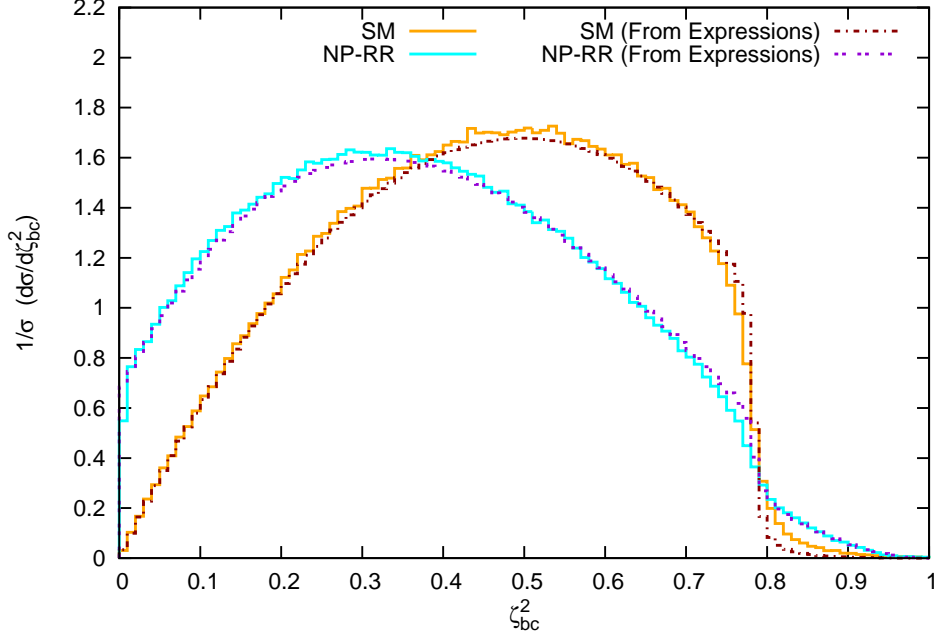


FIG. 2: A comparison of the normalized  $d\sigma/d\zeta_{bc}^2$  distribution obtained using MadGraph 5 with that of Eq. (14). This is done for the SM and for the NP scenario in which  $X_{RR}^S = X_{RR}^V = X_{RR}^T = 1 + i$ , with all other NP parameters set to zero (labelled here as NP-RR).

the decaying particle and converted to its laboratory-frame equivalent by applying a Lorentz boost. At a  $pp$  collider, each event would be associated with a different boost. But since  $\zeta_{ij}^2$  is Lorentz-invariant by construction, the distributions can be expected to look identical in both the top rest frame and the laboratory frame, which is what is seen in Fig. 2.

Note, however, that the observed  $d\sigma/d\zeta_{ij}^2$  distribution is the result of an ensemble of top decays in which the top quarks are not all identical to begin with. While most of the top quarks are produced on-shell, the ensemble also includes top quarks that are off-shell to varying degrees. Moreover, the virtuality of the tops is distributed differently in the fixed-energy and variable-energy cases: in the fixed-energy case one has the additional condition that  $(p_t + p_{\bar{t}})^2$  is fixed. Nevertheless, it turns out that this is a small effect. The normalized distributions for the two cases look almost identical, and the inclusion of PDFs does not lead to any significant change in their shape. The slight (noticeable) difference in the region  $\zeta_{bc}^2 \approx 0.8$  is due to the following. In the analytic expressions, the widths of the  $t$  and the  $W$  are dealt with in slightly different ways. For the  $t$ , the narrow-width approximation is incorporated by making the substitution (see the Appendix)

$$\frac{1}{(p_t^2 - m_t^2)^2 + \Gamma_t^2 m_t^2} \longrightarrow \frac{\pi}{\Gamma_t m_t} \delta(p_t^2 - m_t^2). \quad (25)$$

For the  $W$ , the result of applying the narrow-width approximation is encapsulated in the factor  $\theta(1 - \zeta_W^2 - \zeta_{bc}^2)$  appearing in the definition of  $h_{SM}^{bc}$  in Eq. (13). The finite width of the

$W$  can be approximated to some extent by making the replacement

$$\theta(1 - \zeta_W^2 - \zeta_{bc}^2) \longrightarrow \frac{1}{\pi} \left[ \tan^{-1} \left( \frac{1 - \zeta_W^2 - \zeta_{bc}^2}{\zeta_W \gamma_W} \right) + \tan^{-1} \left( \frac{\zeta_W}{\gamma_W} \right) \right]. \quad (26)$$

This is included in the curves in Fig. 2. On the other hand, in MadGraph 5 both the  $t$  and  $W$  widths are dealt with identically with the integral covering an interval of  $m \pm 15\Gamma$  in each case<sup>6</sup>.

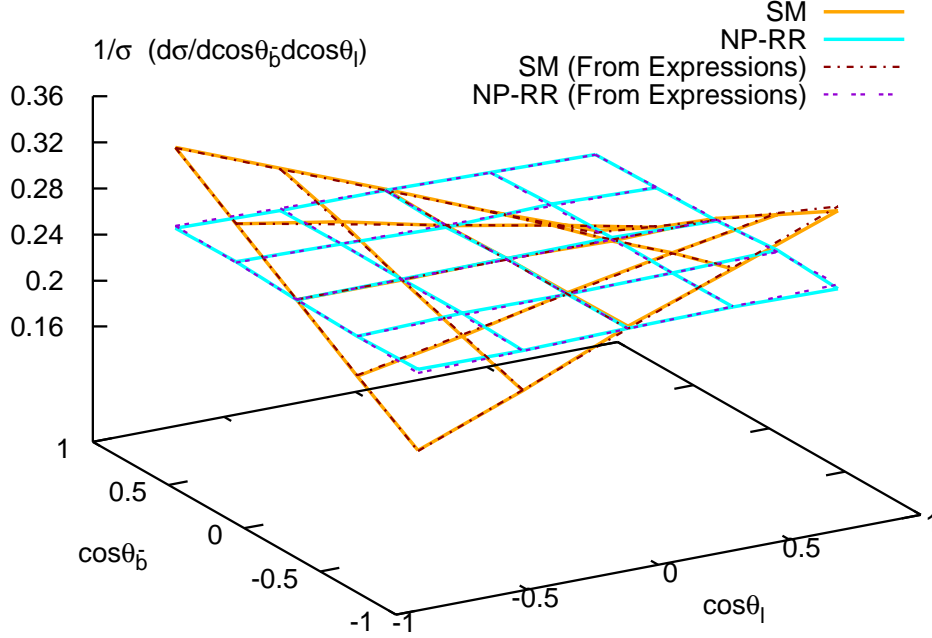


FIG. 3: A comparison of the normalized  $d\sigma/d\cos\theta_b^* d\cos\theta_l^*$  angular distribution obtained using MadGraph 5 with that of Eq. (15). This is done for the SM and for the NP scenario in which  $X_{RR}^S = X_{RR}^V = X_{RR}^T = 1 + i$  (labelled here as NP-RR).

Next we turn to the angular correlation (Fig. 3). This observable involves decay products coming from two different decays. It is therefore sensitive not only to the physics in the two decays (whether new or standard), but also to the correlations in the production of the two decaying particles (i.e., the  $t\bar{t}$  spin correlations). This information is contained in the factor  $\kappa(r)$ . In a fixed-energy gluon-gluon collision,  $\kappa(r)$  is fixed. In our expression [Eq. (15)],  $\kappa(r)$  is replaced by its expectation value  $\langle\kappa(r)\rangle$ . When this is calculated over the energy range sampled in 14 TeV  $pp$  collisions, we find that, once again, the normalized distributions

<sup>6</sup> Within MadGraph 5, this is governed by the parameter `bwcutoff`, which takes the default value 15.

obtained using this expression agree very well with those obtained from the full numerical simulation using MadGraph 5.

The fact that the analytical expressions for the observables agree with numerical simulations suggests that it is possible to extract some of the new-physics parameters by fitting the shapes of these distributions. We present the results of these fits in the companion paper [10]. Note that, in comparing the analytical expressions with the MadGraph 5 simulation, we have taken the  $\bar{b}$  quark to be that coming from the  $t$  decay. However, as noted in the introduction, there is also a  $\bar{b}$  coming from the  $\bar{t}$  decay, and this background must be taken into account. This issue, along with other complications, is addressed in Ref. [10].

## VI. CONCLUSIONS

In this paper we study new-physics (NP) contributions to top-quark decay. Such effects can be significant only for decays that are suppressed in the SM. Here we focus on  $t \rightarrow b\bar{b}c$ , whose SM amplitude involves the small element  $V_{cb}$  ( $\simeq 0.04$ ) of the CKM matrix. Allowing for all Lorentz structures, there are ten possible dimension-6 NP operators that can contribute to this decay. The goal is to find ways of detecting the presence of such NP in  $t \rightarrow b\bar{b}c$ .

Since the LHC produces top quarks copiously, it is an excellent place to search for signals of NP in  $t \rightarrow b\bar{b}c$ . However, the dominant mode for top-quark production is pair ( $t\bar{t}$ ) production via gluon fusion:  $gg \rightarrow t\bar{t}$ . This makes it difficult to study  $t \rightarrow b\bar{b}c$  on its own. In order to search for NP in top decay, the full process  $gg \rightarrow t\bar{t} \rightarrow (b\bar{b}c) (\bar{b}\ell\bar{\nu})$  must be analyzed.

We consider only CP-conserving NP, and find that there are two types of observables that can be used to reveal the presence of NP in top decay. The first is an invariant mass-squared distribution involving two of the final-state particles in  $t \rightarrow b\bar{b}c$ . There are three such distributions. The second is an angular correlation between the decay products of the  $t$  and  $\bar{t}$ . This is related to the  $t\bar{t}$  spin correlation. We consider the angular correlation between one of the final-state quarks in  $t \rightarrow b\bar{b}c$  and the  $\ell^-$  coming from the  $\bar{t}$  decay. There are three such correlations. The six observables depend on different combinations of the coefficients of the ten NP operators.

We compare the analytical expressions for the observables with the results of a numerical simulation of the LHC using MadGraph 5. We find that the agreement between the two is excellent. This suggests that the measurement of these observables can indeed be used to extract some of the new-physics parameters. In the companion paper, Ref. [10], we demonstrate this explicitly by performing fits of such measurements. We also show how to deal with complications such as the background due to the  $\bar{b}$  coming from the  $\bar{t}$  decay.

**Acknowledgments:** The authors wish to thank the MadGraph and FeynRules Teams for extensive discussions about MadGraph and FeynRules, respectively. The authors are also indebted to German Valencia and Howard Baer for helpful discussions and to Zach Bethel and Carl Daudt for technical support. This work was financially supported by NSERC of

Canada (DL, PS). In addition, this work has been partially supported by ANPCyT under grant No. PICT-PRH 2009-0054 and by CONICET (AS). The work of SJ and JM was supported by the U.S. National Science Foundation under Grant PHY-1215785. The work of KK was supported by the U.S. National Science Foundation under Grants PHY-0900914 and PHY-1215785. KK also acknowledges sabbatical support from Taylor University.

## Appendix

In this Appendix we work out an expression for the differential cross section for  $gg \rightarrow t\bar{t} \rightarrow (b\bar{b}c)(\bar{b}\ell\bar{\nu})$ . Our main result may be found below in Eqs. (56)-(59). As an intermediate step, we write the differential cross section for  $gg \rightarrow t\bar{t} \rightarrow (b\bar{b}c)(\bar{b}\ell\bar{\nu})$  in a quasi-factorized form that makes use of expressions for  $gg \rightarrow t\bar{t}$ ,  $t \rightarrow b\bar{b}c$  and  $\bar{t} \rightarrow \bar{b}\ell\bar{\nu}$  (see Eq. (50), below). Throughout, we assume that NP is present only in  $t \rightarrow b\bar{b}c$ ;  $gg \rightarrow t\bar{t}$  and  $\bar{t} \rightarrow \bar{b}\ell\bar{\nu}$  are purely SM in nature. Furthermore, we always employ the narrow-width approximation for the  $t$  and  $\bar{t}$ , which is equivalent to assuming that they are on-shell.

### 1. $gg \rightarrow t\bar{t}$

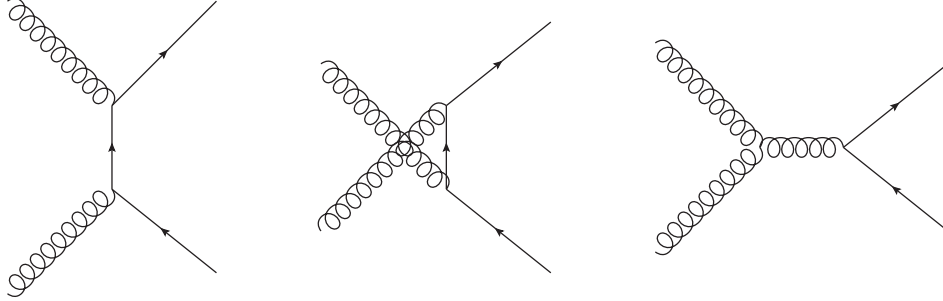


FIG. 4: Feynman diagrams for  $gg \rightarrow t\bar{t}$ . The  $t$  subsequently decays to  $b\bar{b}c$ .

We begin with  $gg \rightarrow t\bar{t}$  (see Fig. 4). The amplitude squared for  $gg \rightarrow t\bar{t}$ , including the  $t$  and  $\bar{t}$  polarizations, was computed in Ref. [17]. It is useful to define the following quantities:<sup>7</sup>

$$P_t \equiv p_t - p_{\bar{t}} , \quad Q \equiv q_1 + q_2 = p_t + p_{\bar{t}} , \quad P_g \equiv q_1 - q_2 , \\ r \equiv \sqrt{1 - 4m_t^2/Q^2} , \quad z \equiv -P_t \cdot P_g / (rQ^2) , \quad (27)$$

where  $p_t$  and  $p_{\bar{t}}$  are the  $t$  and  $\bar{t}$  momenta, and  $q_1$  and  $q_2$  are the momenta of the initial

<sup>7</sup> These definitions are slightly different from those used in Ref. [17].

gluons. The matrix element squared is then given by (see also Fig. 5 and Eq. (32) below),

$$\begin{aligned}
& \frac{1}{256} \sum_{\substack{a,b,i,j; \\ \text{gluon pol'ns}}} |\mathcal{M}^{ab,ij} (gg \rightarrow t(s_t) \bar{t}(s_{\bar{t}}))|^2 \\
&= \frac{g_s^4 (9r^2 z^2 + 7)}{192(r^2 z^2 - 1)^2} \left\{ -f(r, z) + s_t \cdot s_{\bar{t}} g(r, z) \right. \\
&\quad \left. + \frac{r^2(r^2 - 1)(z^2 - 1)}{2m_t^2} [P_g \cdot s_t (P_g \cdot s_{\bar{t}} - Q \cdot s_{\bar{t}} r z) + Q \cdot s_t (P_g \cdot s_{\bar{t}} r z - Q \cdot s_{\bar{t}})] \right\} , \quad (28)
\end{aligned}$$

in which

$$f(r, z) = z^4 r^4 + 2r^2 z^2 (1 - r^2) + 2r^4 - 2r^2 - 1 , \quad (29)$$

$$g(r, z) = r^4 (z^4 - 2z^2 + 2) - 2r^2 + 1 . \quad (30)$$

Integrating the amplitude squared over phase space and summing over the  $t$  and  $\bar{t}$  spins yields the following expression for the parton-level scattering cross-section:

$$\sigma (gg \rightarrow t \bar{t}) = \frac{\pi \alpha_s^2 (1 - r^2)}{192 m_t^2} [r(31r^2 - 59) + 2(r^4 - 18r^2 + 33) \tanh^{-1}(r)] . \quad (31)$$

## 2. Formal Factorization of the Production and Decay Processes.

We now derive expressions that can be used to translate  $t$ -spin-dependent observables into a form that may be more useful to experimentalists. Our starting point is the observation that the spins of the  $t$  and the  $\bar{t}$  are correlated in  $gg \rightarrow t \bar{t}$  [see Eq. (28)]. Thus,  $t$ -spin observables can in principle be translated into observables that employ the spin of the  $\bar{t}$ . This is shown schematically in Fig. 5 (a). Of course, the spin of the  $\bar{t}$  is itself not directly measurable. Fortunately, however, the momentum of the charged lepton in  $\bar{t} \rightarrow \bar{b} \ell \bar{\nu}$  is correlated with the spin of the  $\bar{t}$ . Thus, in order to consider  $t$ -spin-dependent observables in  $t \rightarrow b \bar{b} c$ , we can study the full process  $gg \rightarrow t \bar{t} \rightarrow (b \bar{b} c) (\bar{b} \ell \bar{\nu})$ , as is indicated in Fig. 5 (b).

Consider the two diagrams shown in Fig. 5. The matrices  $A$ ,  $\bar{B}$  and  $C$  indicated there are defined via the production and decay amplitudes as follows:

$$\mathcal{M}^{ab,ij} (gg \rightarrow t(s_t) \bar{t}(s_{\bar{t}})) = \bar{u}_t(p_t, s_t) A^{ab,ij} v_{\bar{t}}(p_{\bar{t}}, s_{\bar{t}}) , \quad (32)$$

$$\mathcal{M}^{iklm} (t(s_t) \rightarrow b \bar{b} c) = \bar{B}^{iklm} u_t(p_t, s_t) , \quad (33)$$

$$\mathcal{M}^{jn} (\bar{t}(s_{\bar{t}}) \rightarrow \bar{b} \ell \bar{\nu}) = \bar{v}_{\bar{t}}(p_{\bar{t}}, s_{\bar{t}}) C^{jn} , \quad (34)$$

in which  $i, j, \dots, n$  are colour indices. We assume that colour indices contract as in the SM, so that

$$\bar{B}^{iklm} = \bar{B} \delta_{ik} \delta_{lm} \quad \text{and} \quad C^{jn} = C \delta_{jn} . \quad (35)$$



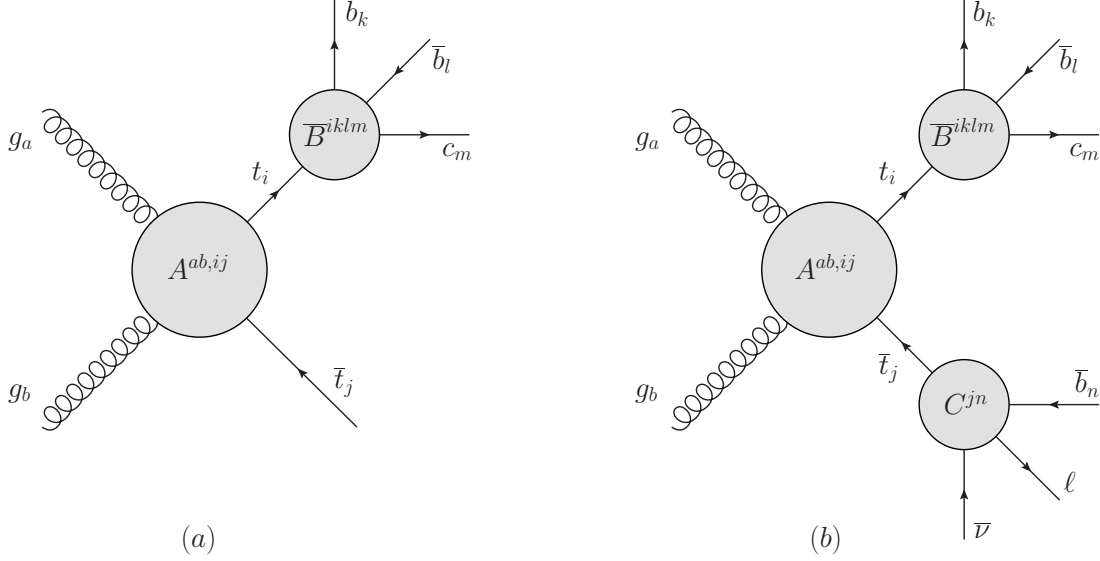


FIG. 5: Feynman diagrams for  $gg \rightarrow t\bar{t} \rightarrow (b\bar{b}c)\bar{t}$  and  $gg \rightarrow t\bar{t} \rightarrow (b\bar{b}c)(\bar{b}\ell\bar{\nu})$ . The subscripts  $i, j, \dots, n$  are colour indices. All NP effects are assumed to be contained in  $\bar{B}$ ;  $gg \rightarrow t\bar{t}$  and  $\bar{t} \rightarrow \bar{b}\ell\bar{\nu}$  are assumed to be SM-like.

Note that  $\bar{B}$  is assumed to contain all of the NP effects. Explicit calculation, starting from the effective Lagrangian given in Eqs (4)-(6), yields

$$\begin{aligned} \bar{B} = 4\sqrt{2}G_F V_{cb}V_{tb} \left[ \frac{1}{2}m_W^2 (\bar{u}_b\gamma_\mu P_L) (\bar{u}_c\gamma^\mu P_L v_{\bar{b}}) G_T (2p_{\bar{b}} \cdot p_c) \right. \\ \left. + X_{LL}^V (\bar{u}_b\gamma_\mu P_L) (\bar{u}_c\gamma^\mu P_L v_{\bar{b}}) + X_{LR}^V (\bar{u}_b\gamma_\mu P_L) (\bar{u}_c\gamma^\mu P_R v_{\bar{b}}) + \dots \right] \end{aligned} \quad (36)$$

Furthermore, we define  $\bar{A}$ ,  $B$  and  $\bar{C}$  via the following relations

$$\bar{A}^{ab,ij} \equiv \gamma^0 (A^{ab,ij})^\dagger \gamma^0, \quad \bar{B} \equiv B^\dagger \gamma^0 \quad \text{and} \quad \bar{C} \equiv C^\dagger \gamma^0. \quad (37)$$

Let us begin by considering the diagram in Fig. 5 (a). The amplitude for this process may be written as follows

$$\mathcal{M}^{ab,klmj}(gg \rightarrow (b\bar{b}c)\bar{t}(s_{\bar{t}})) = -\frac{1}{p_t^2 - m_t^2 + i\Gamma_t m_t} \sum_i \bar{B}^{iklm} (\not{p}_t + m_t) A^{ab,ij} v_{\bar{t}}(p_{\bar{t}}, s_{\bar{t}}). \quad (38)$$

Multiplying the above expression by its complex conjugate and making the substitution

$$\left[ (p_t^2 - m_t^2)^2 + \Gamma_t^2 m_t^2 \right]^{-1} \simeq \frac{\pi}{\Gamma_t m_t} \delta(p_t^2 - m_t^2), \quad (39)$$

we have

$$\begin{aligned}
& \frac{1}{256} \sum_{a,b,k,l,m,j} \sum_{\text{spins}} |\mathcal{M}^{ab,klmj} (gg \rightarrow (b\bar{b}c) \bar{t}(s_{\bar{t}}))|^2 \\
&= \frac{3\pi}{256 \Gamma_t m_t} \sum_{a,b,k,j} \sum_{\text{spins}} \delta(p_t^2 - m_t^2) \\
&\quad \times \frac{1}{2} \text{Tr} \left[ B\bar{B} (\not{p}_t + m_t) A^{ab,kj} (\not{p}_{\bar{t}} - m_t) (1 + \gamma^5 \not{s}_{\bar{t}}) \bar{A}^{ab,kj} (\not{p}_t + m_t) \right], \tag{40}
\end{aligned}$$

where the sum over spins includes the gluon spins as well as those of the  $b$ ,  $\bar{b}$  and  $c$ . Note that the  $t$  quark only shows up via its propagator in this expression. Thus, the spin of the  $t$  is summed over, as it should be. The spin of the  $\bar{t}$ , however, appears explicitly.

This can be simplified by using the following identity, which is similar to an expression in Ref. [18] (see also Ref. [19]):

$$\begin{aligned}
\text{Tr} [\mathbb{X} (\not{p} \pm m) \mathbb{Y} (\not{p} \pm m)] &= \frac{1}{2} \left\{ \text{Tr} [\mathbb{X} (\not{p} \pm m)] \text{Tr} [\mathbb{Y} (\not{p} \pm m)] \right. \\
&\quad \left. - \eta_{\mu\nu} \text{Tr} [\mathbb{X} (\not{p} \pm m) \gamma^5 \gamma^\mu] \text{Tr} [\mathbb{Y} (\not{p} \pm m) \gamma^5 \gamma^\nu] \right\}, \tag{42}
\end{aligned}$$

where

$$\eta_{\mu\nu} \equiv g_{\mu\nu} - \frac{p_\mu p_\nu}{m^2}, \tag{43}$$

and where it is assumed that  $p^2 = m^2$ . Setting

$$\mathbb{X} = B\bar{B}, \tag{44}$$

$$\mathbb{Y} = \frac{1}{2} A^{ab,kj} (\not{p}_{\bar{t}} - m_t) (1 + \gamma^5 \not{s}_{\bar{t}}) \bar{A}^{ab,kj}, \tag{45}$$

we can split the trace in Eq. (41) into two pieces, one corresponding to the  $t\bar{t}$  production ( $\mathbb{Y}$ ) and one to the  $t$  decay ( $\mathbb{X}$ ). Finally, defining

$$n_{t\mu} \equiv -\eta_{\mu\nu} \text{Tr} [B\bar{B} (\not{p}_t + m_t) \gamma^5 \gamma^\nu] / \text{Tr} [B\bar{B} (\not{p}_t + m_t)], \tag{46}$$

we find that we can write the differential cross section corresponding to Fig. 5 (a) in the following suggestive form [18]:

$$d\sigma (gg \rightarrow (b\bar{b}c) \bar{t}(s_{\bar{t}})) = \frac{2}{\Gamma_t} \sum_{b,\bar{b},c \text{ spins}} d\sigma (gg \rightarrow t(n_t) \bar{t}(s_{\bar{t}})) d\Gamma (t \rightarrow b\bar{b}c). \tag{47}$$

Note, however, that there are a few subtleties involved in writing the differential cross section in this way. In particular,

1. The  $t$  polarization,  $n_{t\mu}$ , is a very particular four-vector, defined in Eq. (46).
2. While  $d\sigma (gg \rightarrow t(n_t) \bar{t}(s_{\bar{t}}))$  is calculated for a particular spin four-vector for the  $t$ , the  $t$  spin is averaged in  $d\Gamma (t \rightarrow b\bar{b}c)$ .

3. Although Eq. (47) has the appearance of being factorized cleanly into two pieces, the  $t$ -polarization four-vector contained in  $d\sigma(gg \rightarrow t(n_t)\bar{t}(s_{\bar{t}}))$  depends on the phase-space variables contained in  $d\Gamma(t \rightarrow b\bar{b}c)$ . Similarly, the spin four-vectors for the  $b$ ,  $\bar{b}$  and  $c$  appear both in  $n_{t\mu}$  and in  $d\Gamma(t \rightarrow b\bar{b}c)$ .
4. Given the preceding comment, one must exercise some caution when integrating over phase space and summing over the  $b$ ,  $\bar{b}$  and  $c$  spins. In particular, one must do so for the product of  $d\sigma(gg \rightarrow t\bar{t})$  and  $d\Gamma(t \rightarrow b\bar{b}c)$ , and not for the two quantities separately. For the spin sum, the  $t$ -polarization-dependent quantity that appears in calculations is always  $\text{Tr}[B\bar{B}(\not{p}_t + m_t)]n_{t\mu}$ . It is safe to sum this quantity over spins.

The above approach can be generalized to the scenario indicated in Fig. 5 (b) by applying the trick in Eq. (42) twice in succession, once for the  $t$  and once for the  $\bar{t}$ . One new subtlety in this case is that the final state contains two identical  $\bar{b}$  antiquarks. One should therefore antisymmetrize the total amplitude under the exchange of the two  $\bar{b}$ 's. In practice, we implement cuts in such a way that the two  $\bar{b}$ 's can effectively be distinguished. In particular, in  $t \rightarrow b\bar{b}c$ , we have  $(p_b + p_{\bar{b}} + p_c)^2 = m_t^2$ . But this relation will not, in general, be satisfied if the  $\bar{b}$  comes from the decay of the  $\bar{t}$ . Thus, the two  $\bar{b}$ 's can be distinguished using experimental cuts, and we therefore treat them as non-identical. Further discussion on this point is included in the companion paper [10]. Defining

$$\tilde{n}_{\bar{t}\mu} \equiv -\bar{\eta}_{\mu\nu} \text{Tr}[C\bar{C}(\not{p}_{\bar{t}} - m_t)\gamma^5\gamma^\nu] / \text{Tr}[C\bar{C}(\not{p}_{\bar{t}} - m_t)], \quad (48)$$

where

$$\bar{\eta}_{\mu\nu} \equiv g_{\mu\nu} - \frac{p_{t\mu}p_{t\nu}}{m_t^2}, \quad (49)$$

and proceeding as above, we find [18]

$$\begin{aligned} d\sigma(gg \rightarrow (b\bar{b}c)(\bar{b}\ell\bar{\nu})) \\ = \frac{4}{\Gamma_t^2} \sum_{b,\bar{b},c \text{ spins}} \sum_{\bar{b},\ell,\bar{\nu} \text{ spins}} d\sigma(gg \rightarrow t(n_t)\bar{t}(\tilde{n}_{\bar{t}})) d\Gamma(t \rightarrow b\bar{b}c) d\Gamma(\bar{t} \rightarrow \bar{b}\ell\bar{\nu}). \end{aligned} \quad (50)$$

Use of the above expression requires some care, since the same subtle issues are present as were noted above for the analogous expression in Eq. (47).

### 3. Explicit Expressions for $n_t^\alpha$ and $\tilde{n}_{\bar{t}}^\alpha$

At this stage, let us work out expressions for the “special”  $t$  and  $\bar{t}$  polarization four-vectors,  $n_t^\alpha$  and  $\tilde{n}_{\bar{t}}^\alpha$ , respectively. The quantity that is of interest in the calculation is

$$\begin{aligned} \sum_{b, \bar{b}, c \text{ spins}} \text{Tr}[B\bar{B}(\not{p}_t + m_t)] n_t^\alpha &= -\eta^{\alpha\beta} \sum_{b, \bar{b}, c \text{ spins}} \text{Tr}[B\bar{B}(\not{p}_t + m_t) \gamma^5 \gamma_\beta] \\ &= -\left(4\sqrt{2}G_F V_{tb} V_{cb}\right)^2 \left[ \sum_{i, \sigma} \frac{2 p_i \cdot p_t}{m_t} \left( p_t^\alpha - \frac{m_t^2 p_i^\alpha}{p_i \cdot p_t} \right) \xi^\sigma A_i^\sigma \right. \\ &\quad \left. + 32 m_t \text{Im} \left( X_{LL}^T X_{LL}^{S*} + X_{RR}^T X_{RR}^{S*} \right) \epsilon^{\alpha\beta\gamma\delta} p_{b\beta} p_{\bar{b}\gamma} p_{c\delta} \right]. \end{aligned} \quad (51)$$

Note that this “special” polarization four-vector for the  $t$  quark, which will eventually be incorporated into the expression for  $gg \rightarrow t\bar{t} \rightarrow (b\bar{b}c) (\bar{b}\ell\bar{\nu})$ , contains all of the relevant information and correlations related to the decay of the  $t$ .

Since the semileptonic decay of the  $\bar{t}$  is assumed to be SM-like, the expression for  $\tilde{n}_{\bar{t}}^\alpha$  is much simpler. Defining

$$A_\ell = (p_{\bar{t}} - p_\ell)^2 m_W^4 |G_T(2 p_\ell \cdot p_{\bar{\nu}})|^2, \quad (52)$$

[in analogy with the SM part of Eq. (8)], we find

$$\begin{aligned} \sum_{\bar{b}, \ell, \bar{\nu} \text{ spins}} \text{Tr}[C\bar{C}(\not{p}_{\bar{t}} - m_t)] \tilde{n}_{\bar{t}}^\alpha &= -\bar{\eta}^{\alpha\beta} \sum_{\bar{b}, \ell, \bar{\nu} \text{ spins}} \text{Tr}[C\bar{C}(\not{p}_{\bar{t}} - m_t) \gamma^5 \gamma_\beta] \\ &= \left(4\sqrt{2}G_F V_{tb}\right)^2 \frac{2 p_\ell \cdot p_{\bar{t}}}{m_t} \left( p_{\bar{t}}^\alpha - \frac{m_t^2 p_\ell^\alpha}{p_\ell \cdot p_{\bar{t}}} \right) A_\ell. \end{aligned} \quad (53)$$

Equations (51) and (53) may be compared to related expressions in Ref. [19]. The following expressions are also useful:

$$\sum_{b, \bar{b}, c \text{ spins}} \text{Tr}[B\bar{B}(\not{p}_t + m_t)] = \left(4\sqrt{2}G_F V_{tb} V_{cb}\right)^2 \sum_{i, \sigma} 2 p_i \cdot p_t A_i^\sigma, \quad (54)$$

$$\sum_{\bar{b}, \ell, \bar{\nu} \text{ spins}} \text{Tr}[C\bar{C}(\not{p}_{\bar{t}} - m_t)] = \left(4\sqrt{2}G_F V_{tb}\right)^2 2 p_\ell \cdot p_{\bar{t}} A_\ell. \quad (55)$$

With these expressions in hand, we can now work out the final expression for the differential cross-section.

### 4. Differential cross-section

Using Eqs. (51) and (53) in Eq. (50), we have

$$d\sigma(gg \rightarrow t\bar{t} \rightarrow (b\bar{b}c) (\bar{b}\ell\bar{\nu})) = (\mathcal{B}_{\text{non-TP}} + \mathcal{B}_{\text{TP}}) d\lambda, \quad (56)$$

where

$$\begin{aligned} \mathcal{B}_{\text{non-TP}} = \sum_{i,\sigma} A_i^\sigma A_\ell \Big\{ & - \frac{p_i \cdot p_t p_\ell \cdot p_{\bar{t}}}{m_t^2} [f(r, z) + \xi^\sigma (r^4 (z^4 - 2) + 1)] - \xi^\sigma p_i \cdot p_\ell g(r, z) \\ & - \frac{(r^2 - 1) [r^2 (z^2 - 2) + 1] \xi^\sigma}{2m_t^2} (p_i \cdot Q Q \cdot p_\ell + p_i \cdot P_t P_t \cdot p_\ell) \\ & - \frac{r^2 (r^2 - 1) (z^2 - 1) \xi^\sigma}{2m_t^2} [p_i \cdot P_g (P_g \cdot p_\ell - Q \cdot p_\ell r z) \\ & + p_i \cdot Q (P_g \cdot p_\ell r z - Q \cdot p_\ell)] \Big\}, \end{aligned} \quad (57)$$

$$\begin{aligned} \mathcal{B}_{\text{TP}} = 16 A_\ell \text{Im} (X_{LL}^T X_{LL}^{S*} + X_{RR}^T X_{RR}^{S*}) \Big\{ & - g(r, z) \epsilon(p_b, p_{\bar{b}}, p_c, p_\ell) \\ & - \frac{(r^2 - 1) p_\ell \cdot p_{\bar{t}}}{m_t^2} [r^2 (z^2 - 2) + 1] \epsilon(p_b, p_{\bar{b}}, p_c, Q) \\ & - \frac{r^2 (r^2 - 1) (z^2 - 1)}{2m_t^2} [(P_g \cdot p_\ell - Q \cdot p_\ell r z) \epsilon(p_b, p_{\bar{b}}, p_c, P_g) \\ & + (P_g \cdot p_\ell r z - Q \cdot p_\ell) \epsilon(p_b, p_{\bar{b}}, p_c, Q)] \Big\}, \end{aligned} \quad (58)$$

and

$$\begin{aligned} d\lambda = & \frac{\alpha_S^2 G_F^4 V_{tb}^4 V_{cb}^2 (1 - r^2) r}{4 (4\pi)^{10} \Gamma_t^2 m_t^2} \left(1 - \frac{M_2^2}{m_t^2}\right) \left(1 - \frac{M_5^2}{m_t^2}\right) \frac{(9r^2 z^2 + 7)}{(r^2 z^2 - 1)^2} \\ & \times dM_2^2 dM_5^2 d\Omega_1^{**} d\Omega_2^* d\Omega_4^{**} d\Omega_5^* d\Omega_t. \end{aligned} \quad (59)$$

In the above, the  $p_i$  are the momenta of the final-state quarks coming from the top decay (i.e.,  $b$ ,  $\bar{b}$  and  $c$ ); also,  $P_t$ ,  $Q$ ,  $P_g$ ,  $r$ ,  $z$ ,  $f(r, z)$  and  $g(r, z)$  were defined in Eqs. (27), (29) and (30). In arriving at the above expression for  $d\lambda$ , we have decomposed the six-body phase space into five solid angles and four invariant masses (see Fig. 1), and then have used the narrow-width approximation for the  $t$  and  $\bar{t}$  quarks to eliminate two of the invariant-mass degrees of freedom. The solid angles  $d\Omega_1^{**}$ - $d\Omega_t$  and the invariant masses  $M_2$  and  $M_5$  are discussed in Sec. III.

Inspection of Eqs. (57) and (58) reveals elements that are a combination of expressions coming from the production and decay of the  $t$  and  $\bar{t}$  quarks. The  $A_i^\sigma$  are related to the decay  $t \rightarrow b\bar{b}c$  [see Eqs. (8)-(10)].  $A_\ell$  is similarly related to the semileptonic decay of the  $\bar{t}$ .

## 5. Integrated cross-section

In the SM,

$$\begin{aligned} \sigma_{\text{SM}} & \equiv \sigma(gg \rightarrow t\bar{t} \rightarrow (b\bar{b}c)(\bar{b}\ell\bar{\nu}))|_{\text{SM}} \\ & = \sigma(gg \rightarrow t\bar{t}) \text{BR}(t \rightarrow b\bar{b}c)|_{\text{SM}} \text{BR}(\bar{t} \rightarrow \bar{b}\ell\bar{\nu}), \end{aligned} \quad (60)$$

in which  $\sigma(gg \rightarrow t\bar{t})$  is defined in Eq. (31),  $\text{BR}(t \rightarrow b\bar{b}c)|_{\text{SM}} = V_{tb}^2 V_{cb}^2 / 3$  and  $\text{BR}(\bar{t} \rightarrow \bar{b}\ell\bar{\nu}) = V_{tb}^2 / 9$ .

After the inclusion of new physics,

$$\begin{aligned}
\sigma_{\text{SM+NP}} &\equiv \sigma \left( gg \rightarrow t\bar{t} \rightarrow (b\bar{b}c) (\bar{b}\ell\bar{\nu}) \right) |_{\text{SM+NP}} \\
&= \sigma_{\text{SM}} \left\{ 1 + \frac{4\Gamma_W}{m_W} \text{Im} \left( X_{LL}^{V*} \right) + \frac{3G_F m_t^2}{4\sqrt{2}\pi^2 (1 - \zeta_W^2)^2 (1 + 2\zeta_W^2)} \sum_{i,\sigma} \hat{A}_i^\sigma \right\}. \quad (61)
\end{aligned}$$

- 
- [1] V. M. Abazov *et al.* [D0 Collaboration], Phys. Rev. D **85**, 091104 (2012) [arXiv:1201.4156 [hep-ex]]; T. A. Aaltonen *et al.* [CDF Collaboration], Phys. Rev. Lett. **111**, 202001 (2013) [arXiv:1308.4050 [hep-ex]].
  - [2] G. Aad *et al.* [ATLAS Collaboration], Phys. Lett. B **717**, 330 (2012) [arXiv:1205.3130 [hep-ex]].
  - [3] K. Kiers, T. Knighton, D. London, M. Russell, A. Szynekman and K. Webster, Phys. Rev. D **84**, 074018 (2011) [arXiv:1107.0754 [hep-ph]].
  - [4] K. Kiers, D. London, P. Saha and A. Szynekman, in preparation.
  - [5] *Experimental measurements of the  $t\bar{t}$  spin correlation involving four jets can be found in* T. Aaltonen *et al.* [CDF Collaboration], Phys. Rev. D **83**, 031104 (2011) [arXiv:1012.3093 [hep-ex]]; V. M. Abazov *et al.* [D0 Collaboration], Phys. Rev. Lett. **108**, 032004 (2012) [arXiv:1110.4194 [hep-ex]]; G. Aad *et al.* [ATLAS Collaboration], arXiv:1407.4314 [hep-ex].  
*The CMS Collaboration has made a measurement using two jets:*  
S. Chatrchyan *et al.* [CMS Collaboration], Phys. Rev. Lett. **112**, 182001 (2014) [arXiv:1311.3924 [hep-ex]].
  - [6] G. Mahlon and S. J. Parke, Phys. Rev. D **81**, 074024 (2010) [arXiv:1001.3422 [hep-ph]].
  - [7] M. Arai, N. Okada, K. Smolek and V. Simak, Phys. Rev. D **70**, 115015 (2004) [hep-ph/0409273]; M. Arai, N. Okada, K. Smolek and V. Simak, Phys. Rev. D **75**, 095008 (2007) [hep-ph/0701155]; R. Frederix and F. Maltoni, JHEP **0901**, 047 (2009) [arXiv:0712.2355 [hep-ph]]; M. Arai, N. Okada and K. Smolek, Phys. Rev. D **79**, 074019 (2009) [arXiv:0902.0418 [hep-ph]]; C. -X. Yue, T. -T. Zhang and J. -Y. Liu, J. Phys. G **37**, 075016 (2010) [arXiv:1003.2770 [hep-ph]]; C. Degrande, J. -M. Gerard, C. Grojean, F. Maltoni and G. Servant, JHEP **1103**, 125 (2011) [arXiv:1010.6304 [hep-ph]]; J. Cao, L. Wu and J. M. Yang, Phys. Rev. D **83**, 034024 (2011) [arXiv:1011.5564 [hep-ph]]; M. Baumgart and B. Tweedie, JHEP **1109**, 049 (2011) [arXiv:1104.2043 [hep-ph]]; D. Krohn, T. Liu, J. Shelton and L. -T. Wang, Phys. Rev. D **84**, 074034 (2011) [arXiv:1105.3743 [hep-ph]]; Y. Bai and Z. Han, JHEP **1202**, 135 (2012) [arXiv:1106.5071 [hep-ph]]; V. Barger, W. -Y. Keung and B. Yencho, Phys. Rev. D **85**, 034016 (2012) [arXiv:1112.5173 [hep-ph]]; S. Fajfer, J. F. Kamenik and B. Melic, JHEP **1208**, 114 (2012) [arXiv:1205.0264 [hep-ph]]; Z. Han, A. Katz, D. Krohn and M. Reece, JHEP **1208**, 083 (2012) [arXiv:1205.5808 [hep-ph]]; M. Baumgart and B. Tweedie, JHEP **1303**, 117 (2013) [arXiv:1212.4888 [hep-ph]].
  - [8] D. Atwood, A. Aeppli and A. Soni, Phys. Rev. Lett. **69**, 2754 (1992); W. Bernreuther and A. Brandenburg, Phys. Rev. D **49**, 4481 (1994) [hep-ph/9312210]; K. -m. Cheung, Phys. Rev. D **55** (1997) 4430 [hep-ph/9610368]; H. -Y. Zhou, Phys. Rev. D **58**, 114002 (1998) [hep-ph/9805358]; M. Beneke, I. Efthymiopoulos, M. L. Mangano, J. Womersley, A. Ahmadov, G. Azuelos, U. Baur and A. Belyaev *et al.*, In \*Geneva 1999, Standard model physics (and more) at the LHC\* 419-529 [hep-ph/0003033]; O. Antipin and G. Valencia, Phys. Rev. D **79**, 013013 (2009) [arXiv:0807.1295 [hep-ph]]; S. K. Gupta, A. S. Mete and G. Valencia, Phys. Rev. D **80**, 034013 (2009) [arXiv:0905.1074 [hep-ph]]; S. K. Gupta and G. Valencia, Phys. Rev. D **81**, 034013 (2010) [arXiv:0912.0707 [hep-ph]]. X. -G. He, G. Valencia and H. Yokoya, JHEP **1112**, 030 (2011) [arXiv:1110.2588 [hep-ph]].
  - [9] T. Aaltonen *et al.* [CDF Collaboration], Phys. Rev. D **83**, 112003 (2011) [arXiv:1101.0034 [hep-]]

- ex]]; V. M. Abazov *et al.* [D0 Collaboration], Phys. Rev. D **84**, 112005 (2011) [arXiv:1107.4995 [hep-ex]].
- [10] P. Saha, K. Kiers, D. London and A. Szynekman, arXiv:1407.1725 [hep-ph].
  - [11] A. Datta and D. London, Phys. Lett. B **595**, 453 (2004) [hep-ph/0404130].
  - [12] E. Byckling and K. Kajantie, *Particle Kinematics* (Wiley, New York, 1973).
  - [13] N. Kidonakis, arXiv:1304.7775 [hep-ph]; S. Moch and P. Uwer, Phys. Rev. D **78**, 034003 (2008) [arXiv:0804.1476 [hep-ph]].
  - [14] J. Alwall, M. Herquet, F. Maltoni, O. Mattelaer and T. Stelzer, JHEP **1106**, 128 (2011) [arXiv:1106.0522 [hep-ph]]; <http://madgraph.hep.uiuc.edu/>.
  - [15] A. Alloul, N. D. Christensen, C. Degrande, C. Duhr and B. Fuks, Comput. Phys. Commun. **185**, 2250 (2014) [arXiv:1310.1921 [hep-ph]]. <http://feynrules.irmp.ucl.ac.be/>.
  - [16] J. Pumplin, D. R. Stump, J. Huston, H. L. Lai, P. M. Nadolsky and W. K. Tung, JHEP **0207**, 012 (2002) [hep-ph/0201195]. <http://hep.pa.msu.edu/cteq/public/cteq6.html>.
  - [17] D. Atwood, A. Aeppli, A. Soni, Ref. [8].
  - [18] S. Kawasaki, T. Shirafuji and S. Y. Tsai, Prog. Theor. Phys. **49**, 1656 (1973).
  - [19] T. Arens and L. M. Sehgal, Phys. Rev. D **50**, 4372 (1994).